

Fig. 2. Schematic structure of the low-finesse A-FPSA designed for 1.51  $\mu\text{m}$ . LT, low-temperature MBE growth; MQW, multiple quantum well

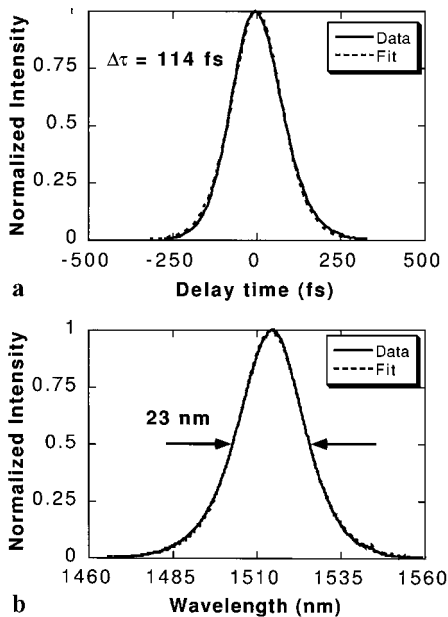


Fig. 3. **a** Background-free intensity autocorrelation and **b** corresponding spectral profile from a soliton-modelocked Cr(4+):YAG laser. Dashed curves are fits in which a sech pulse shape is assumed

For both continuous wave (cw) and pulsed operation we obtain the best results with 1.7% output coupling at one end of the cavity. At a pump power of 7.8 W, 6 W of which is absorbed, the maximum output power is 1.21 W for cw operation. The cw threshold pump power is at 1.1 W, i.e. at 0.88 W absorbed power. For pulsed operation the highly reflecting end mirror is replaced by the A-FPSA with a 100-mm-curved mirror providing a 45  $\mu\text{m}$  focal waist at the absorber (Fig. 1).

Our A-FPSA consists of four low-temperature (350  $^{\circ}\text{C}$ ) molecular-beam-epitaxy-grown  $\text{In}_x\text{Ga}_{1-x}\text{As}/\text{GaAs}$  ( $x = 0.53$ ) quantum wells on an AlAs/GaAs Bragg mirror (Fig. 2). The saturable absorber front side is uncoated, resulting in a low finesse A-FPSA with a broadband low-intensity reflectivity centered at 1540 nm, a measured modulation depth of  $(0.7 \pm 0.2)\%$ , and an unsaturated insertion loss of about  $(2.2 \pm 0.2)\%$ . The saturation intensity is approximately  $0.7 \text{ pJ}/\mu\text{m}^2$ .

In a pump-probe setup the A-FPSA time response is found to be bitemporal with a fast recovery time of 0.5 ps and a slow one of 12 ps.

Without any elements for group-velocity-dispersion (GVD) compensation inside the cavity, we observe self-starting but also strongly chirped pulses with pulse widths of 6–8 ps. If a fused-silica Brewster-prism pair with particularly low water content is inserted into the cavity, the pulse width is reduced substantially. At a tip-to-tip prism separation of 155 mm, the shortest pulses from self-starting long-term stable operation of the laser were observed at an average output power of 94 mW and a repetition rate of 185 MHz (Fig. 3). The measured intensity autocorrelation trace is fitted by assuming a hyperbolic secans pulse shape, which yields pulse widths as short as 114 fs (FWHM) (Fig. 3a). The spectral width is 23 nm (FWHM) centered at 1514 nm (Fig. 3b). The resulting time–bandwidth product of  $0.34 \pm 0.01$  indicates transform-limited pulses, which are also confirmed by a chirpfree interferometric autocorrelation trace.

For the pulses described above we verified that a single pulse was present in the laser cavity. As in the observations reported previously for Nd:glass lasers [12], a breakup into several pulses was observed at increased intracavity energy. The pulse train was monitored by a fast 6.5 GHz photodiode and a 6.5 GHz spectrum analyser. Shorter pulse separations were measured by the analysis of modulations in the optical spectrum. With the grating inside our monochromator (68 mm  $\times$  68 mm, 600 lines/mm) fully illuminated its resolution was 5.5 GHz. Therefore all frequencies from zero up to the optical frequency were covered. In addition, the autocorrelation allowed us to observe pulse separations of up to 1 ps. The measured spacing between the pulses ranged from 700 fs up to half the cavity roundtrip time. In multiple pulse operation the maximum output power was 395 mW when the measured average autocorrelation width was 185 fs (FWHM). The autocorrelation trace can be best fitted by assuming 120 fs sech-shaped pulses. However, as the individual pulses are averaged in the autocorrelation trace they need not be of equal width and energy. The shortest multiple pulses were fitted yielding 95 fs (FWHM) by again assuming a sech pulse shape.

In order to explain the modelocking mechanism in our system, we first consider the A-FPSA. In the case of low modulation depth, as for our A-FPSA, the minimum unchirped pulse width is expected to coincide more or less with the fast response time in a model of a pure fast saturable absorber [13]. Without prisms we find picosecond pulses with a strong chirp, which is mainly caused by the positive GVD of the Cr(4+):YAG crystal [4]. With the prisms inserted we observe pulses that are shorter than the fast recovery time – the reduction factor lying between 4 and 5. Therefore we conclude that femtosecond modelocking of our Cr(4+):YAG laser is not caused by the A-FPSA alone.

Another modelocking mechanism to be checked is Kerr-lens modelocking (KLM), which has been applied to most of the femtosecond Cr(4+):YAG lasers realized so far [2–5]. First we replaced the A-FPSA by a high reflector and tried to induce soft-aperture modelocking mechanically, but with no success. With the A-FPSA inserted back into the cavity, the laser was operated at various spacings between the absorber and its focusing mirror. All along the cavity stability range, self-starting modelocking was observed. This is not

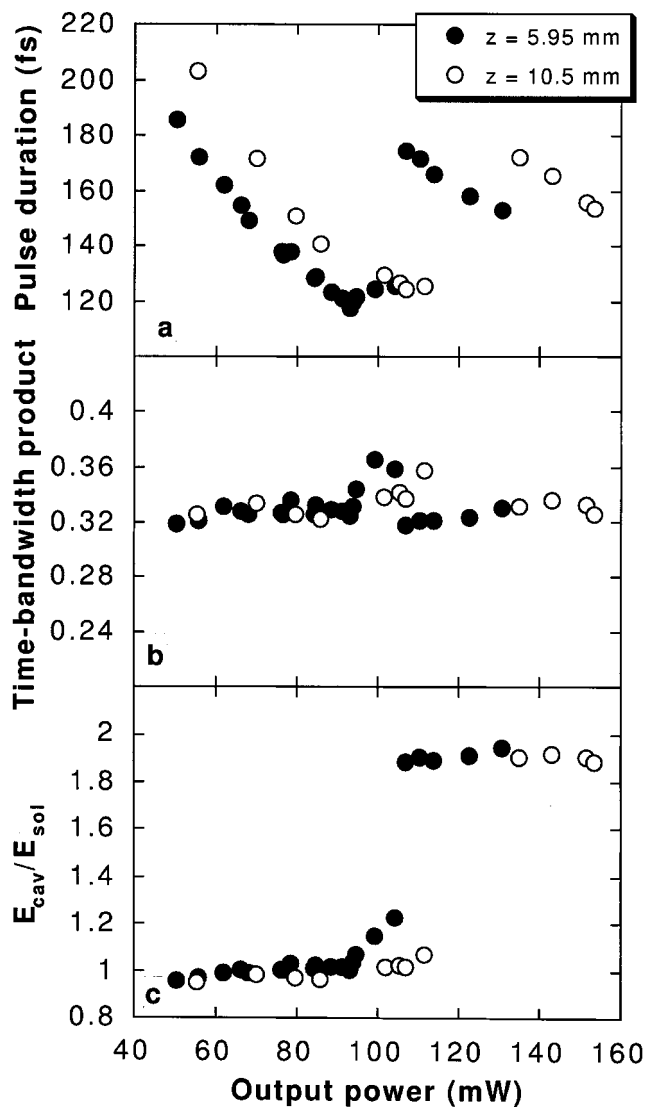


**Fig. 4a–c.** Analysis of the intracavity soliton dynamics. Filled circles correspond to a lateral prism insertion of  $z = 5.95$  mm, hollow circles to  $z = 10.5$  mm. As a function of average output power, the figure shows **a** the pulse duration at FWHM with a sech pulse shape assumed, **b** the corresponding time-bandwidth product and **c** the total intracavity energy normalised to the soliton energy. The tip-to-tip prism separation, repetition rate, and spot size on the absorber were at 235 mm, 162.5 MHz, and 35  $\mu\text{m}$ , respectively

expected at all for KLM, which should be critically dependent on the cavity parameters [14] and should appear only close to the borders of the stability range. This is confirmed by ABCD matrix calculations, which result in an insignificant KLM contribution for our cavity. Therefore, we exclude KLM as responsible for pulse formation in our Cr(4+):YAG laser system.

We demonstrate that the dominant modelocking mechanism for our femtosecond Cr:YAG laser is soliton modelocking [9], which is explained as follows. In the steady state, both a soliton pulse and a low-intensity continuum background exist inside the cavity. Without a saturable absorber the continuum experiences higher gain than the soliton, because it sees only the gain at the line center, whereas the soliton experiences an effectively lower average gain because of its larger

bandwidth. Thus the continuum would grow and eventually de-stabilize the soliton. By introducing the saturable absorber we add high loss for the continuum but only negligible loss for the intense soliton pulse. Therefore, even a slow saturable absorber stabilizes the soliton against the continuum.

In order to verify the soliton-modelocking model and to understand the multiple pulsing of the laser, the pulse durations and spectral widths were analysed as follows.

Figure 4a shows the variation of the pulse width with increasing output power. Solitons scale their pulse width inversely proportionally to the pulse energy. This functional relation is approximately fulfilled for single pulses up to 95 mW at a lateral prism insertion of  $z = 5.95$  mm (up to 110 mW at  $z = 10.5$  mm). At higher output powers another branch of inverse proportional scaling is observed, similar to what has been reported previously for Nd:glass lasers [12], where it has been attributed to double and multiple pulses inside the laser cavity. It is important to note that exact inverse proportional scaling of pulse duration versus pulse energy, as expected for solitons, requires constant dispersion and center wavelength. Additional data, not shown here, indicate a variation of the center wavelength with pulse energy, resulting in a dispersion variation of up to 10%.

The time-bandwidth product shown in Fig. 4b indicates that transform-limited pulses exist in both branches except near the single-to-multiple pulse transition around 100 mW output power, where the breaking-up of the pulses was anticipated by the appearance of continuous wave peaks in the pulse spectra.

In order to assess the multiple pulsing regime of operation, the total intracavity energy  $E_{cav}$  relative to the soliton energy  $E_{sol}$  is shown in Fig. 4c. Here the change in dispersion due to center wavelength variations was taken into account. By assuming single solitons for output powers up to 95 mW (110 mW) for  $z = 5.95$  mm ( $z = 10.5$  mm), both the residual cavity dispersion and the effective crystal nonlinearity were determined to fit the soliton intracavity energy [9]. With the same fitting parameters applied to pulses at power levels above 100 mW, the intracavity energy almost doubles relative to the soliton energy, which strongly suggests that two solitons of approximately equal amplitude circulate in the laser. Therefore, the branch beyond 100 mW must be interpreted as double-pulsed soliton-modelocked operation of the laser.

The single-to-multiple pulse transitions correspond to intensities incident on the absorber of more than a factor of 10 above the A-FPSA saturation intensity. As a consequence, the absorber reflectivity is only insignificantly modified if a single pulse breaks up into two, and its discrimination between single and multiple pulsing is reduced substantially [12]. In addition, the finite-gain bandwidth experienced by the pulses may favour multiple intracavity solitons with reduced spectral width compared to a single broadband soliton [12].

So by using an A-FPSA, we have achieved self-starting transform-limited femtosecond pulsed operation for a Cr(4+):YAG laser. Long-term stable 114 fs pulses centered at 1.5  $\mu\text{m}$  were observed at 94 mW average output power. Soliton modelocking means that the pulse widths are continuously tunable from 115 fs up to 205 fs. Pulse energies of up to 0.66 nJ were measured; the corresponding peak power of 4.7 kW causes enough nonlinear response in a typical optical fiber to produce solitons in the 100 fs range. Aiming at high pulse energy, we found that the onset of multiple pulsing

is displaced by increasing the amount of negative group-velocity dispersion in the cavity. Alternatively, the energy per pulse may be increased either by reducing the incident intensity on the A-FPSA, e.g. by increasing the spot size on the absorber, or by a modified absorber design with increased saturation intensity. Moreover, multiple pulses equally spaced by fractions of the cavity roundtrip length are observed in our Cr(4+):YAG laser, which is interesting for a gigahertz-repetition-rate femtosecond laser source at the telecommunication wavelength 1.5  $\mu\text{m}$ . Their stabilisation will be further investigated.

*Acknowledgements.* The authors thank J.R. Taylor, K. Bergman, F.X. Kärtner, F. König and U. Ströbner for helpful discussions. The research was supported by an EU grant, project number 20029 (ACQUIRE), in the framework of ESPRIT.

## References

1. A.V. Shestakov, N.I. Borodin, V.A. Zhitnyuk, A.G. Ohrimtchuk, V.P. Gapontsev: In *Digest of Conference on Lasers and Electro-Optics* (Optical Society of America, Washington, DC 1991), paper CPDP11
2. A. Sennaroglu, C.R. Pollock, H. Nathel: *Opt. Lett.* **19**, 390 (1994); A. Sennaroglu, C.R. Pollock, H. Nathel: In *Digest of Meeting on Advanced Solid-State Lasers* (Optical Society of America, Washington, DC 1994) pp. 4–6
3. P.J. Conlon, Y.P. Tong, P.M.W. French, J.R. Taylor, A.V. Shestakov: *Opt. Lett.* **19**, 1468 (1994)
4. Y. Ishida, K. Naganuma: *Opt. Lett.* **19**, 2003 (1994)
5. Y.P. Tong, J.M. Sutherland, P.M.W. French, J.R. Taylor, A.V. Shestakov, B.H.T. Chai: *Opt. Lett.* **21**, 644 (1996)
6. U. Keller, D.A.B. Miller, G.D. Boyd, T.H. Chiu, J.F. Ferguson, M.T. Asom: *Opt. Lett.* **17**, 505 (1992); U. Keller, K.J. Weingarten, F.X. Kärtner, D. Kopf, B. Braun, I.D. Jung, R. Fluck, C. Hönninger, N. Matuschek, J. Aus der Au: *IEEE J. Selected Topics in Quantum Electronics (JSTQE)* **3**, 435 (1996)
7. L.R. Brovelli, U. Keller, T.H. Chiu: *J. Opt. Soc. Am. B* **12**, 311 (1995)
8. B.C. Collings, J.B. Stark, S. Tsuda, W.H. Knox, J.E. Cunningham, W.Y. Jan, R. Pathak, K. Bergman: *Opt. Lett.* **21**, 1171 (1996)
9. F.X. Kärtner, U. Keller: *Opt. Lett.* **20**, 16 (1995)
10. I.D. Jung, F.X. Kärtner, L.R. Brovelli, M. Kamp, U. Keller: *Opt. Lett.* **20**, 1892 (1995)
11. R. Fluck, I.D. Jung, G. Zhang, F.X. Kärtner, U. Keller: *Opt. Lett.* **21**, 743 (1996)
12. J. Aus der Au, D. Kopf, F. Morier-Genoud, M. Moser, U. Keller: *Opt. Lett.* **22**, 307 (1997)
13. H.A. Haus, J.G. Fujimoto, E.P. Ippen: *J. Opt. Soc. Am. B* **8**, 2068 (1991)
14. G. Cerullo, S. De Silvestri, V. Magni, L. Pallaro: *Opt. Lett.* **19**, 807 (1994)